Available online at www.sciencedirect.com
SCIENCE DIRECT®
Journal of Catalysis 227 (2004) 33–43
JOURNAL OF CATALYSIS
www.elsevier.com/locate/jcat

# *trans*-1,2-Dichloroethene on $Cu_{50}Pd_{50}(110)$ alloy surface: dynamical changes in the adsorption, reaction, and surface segregation

L.H. Bloxham [a], S. Haq [a], Y. Yugnet [b], J.C. Bertolini [b], R. Raval [a,*]

[a] *Surface Science Research Centre, Department of Chemistry, University of Liverpool, Liverpool, L69 3BX, UK*
[b] *Institut de Recherches sur la Catalyse/CNRS, 2, ave. A. Einstein, F-69626, Villeurbanne cedex, France*

Received 16 April 2004; revised 10 June 2004; accepted 13 June 2004

Available online 20 July 2004

**Abstract**

The adsorption and reaction of *trans*-1,2-dichloroethene on CuPd(110) have been studied using molecular beam adsorption reaction, temperature-programmed desorption, reflection absorption infrared, high-resolution electron energy loss, and X-ray photoelectron spectroscopies. Below 165 K, the molecules adsorb intact at all coverages with their molecular planes orientated largely parallel to the metal surface. Above 165 K, decomposition is observed initially on adsorption, but is limited by availability of surface sites and stablisation effects of coadsorbed Cl. Between 300 and 350 K the main desorbing decomposition products are $H_2$ and $C_2H_2$, while only $H_2$ is produced between 350 and 675 K. Above 675 K evolution of HCl is observed. The decomposition of the hydrocarbon skeleton occurs mainly at Pd sites, while dechlorination is catalysed at Cu sites with Cl preferentially binding to the Cu atoms. This leads to dynamic changes in surface composition of the alloy with segregation of underlying Cu atoms to the surface that scavenge the Cl atoms and thus help to keep the Pd sites Cl free.


*Keywords:* Reactions at surfaces; *trans*-1,2-Dichloroethene; CuPd(110); TPD; RAIRS; HREELS; XPS; Molecular beam; HCl; $C_2H_2$

## 1. Introduction

Hydrodechlorination is a key reaction in the processing of many potentially harmful chlorinated compounds [1–6]; it essentially involves the hydrogenolysis of the C–Cl bond using a catalyst ($RC–Cl + H_2 \rightarrow RC–H + HCl$). This reaction has distinct advantages over more traditional methods of chlorinated waste disposal: the hydrocarbon products can be recycled as fuel or chemical feedstocks, the HCl can be separated and neutralized, and harmful products like $Cl_2$, $COCl_2$, or chlorocarbon fragments are not produced [7]. Of the many materials tested as potential catalysts for this reaction [3,6–12], Group VIII transition metals have been found to be the most suitable in terms of activity, selectivity, and stability [3,6,7]. Due to its affinity to chlorine, Cu could also be an effective agent for C–Cl bond cleavage [12]; however, the use of Cu as an effective dechlorination catalyst is limited by its inability to remove surface chlorine, which can ultimately poison the catalyst. Addition of a second metal capable of performing this function has proved to be an effective solution and research has shown that CuPd binary alloys are particularly good catalysts for the reaction, exhibiting superior activity and selectivity to either of the pure components [13]. To gain a detailed insight into the physical basis for the enhanced activity and selectivity of CuPd bimetallic catalysts, we have been studying the adsorption of simple chloroethenes on well-defined Pd(110) [14], Cu(110) [15–18], and CuPd(110) [19–21] surfaces. With this systematic approach and with detailed comparisons, an understanding of how the initial reactant molecular structure and metallic composition of a surface direct the reaction pathway can be formulated.

The adsorption and reaction of chloroethenes have been studied on the Cu(110) [15–18], Cu(100) [22], Pt(111)

* Corresponding author.
*E-mail address:* r.raval@liv.ac.uk (R. Raval).

0021-9517/$ – see front matter 
doi:10.1016/j.jcat.2004.06.015

[23–25], Pd(100) [26], Pd(110) [14], and CuPd [27–29] surfaces. The adsorption of *trans*-1,2-dichloroethene on Cu(110) and Pd(110) surfaces is briefly reviewed as it is directly relevant to this work. The reaction of *trans*-1,2-dichloroethene on Pd(110) shows complex changes as a function of substrate temperature and reactant coverage, for which five distinct reaction regimes have been identified [14]. At low temperatures (85–130 K, *Regime I*), intact molecular adsorption is observed in both the monolayer and the multilayers. Above this temperature decomposition is observed from the onset of adsorption and the nature of the surface and desorbing species is critically affected by the uptake and temperature. Between 180 and 220 K (*Regime II*), initial total decomposition is followed by selective dechlorination to produced adsorbed acetylene. Evolution of gas-phase products starts at 250 K, and for low uptake values over the temperature range 250–675 K (*Regime III*) $H_2$ is liberated into the gas phase. At high uptake values between 250 and 360 K (*Regime IV*) $C_2H_2$ and HCl are the main desorbing reaction products. Finally, in *Regime V*, a pseudo-steady-state evolution of gaseous HCl is observed, which begins at 390 K for high uptake values or above 670 K from the onset of adsorption. These changes in the reaction behaviour of *trans*-1,2-dichloroethene on the Pd(110) surface were attributed to dynamic changes in (i) the ability of the surface to dissociate C–H and C–Cl bonds and (ii) in the barriers to product evolution as the temperature and surface contamination of the system are varied.

The reaction of *trans*-1,2-dichloroethene on Cu(110) shows no desorbing HCl or chlorocarbon reaction products [17]. Below 170 K molecular adsorption is observed. A competing molecular desorption and dehalogenation process begins at 170 K, in which a self-poisoning reaction leads to desorption of intact molecular species at 171 and 260 K, while the competing dechlorination reaction produces adsorbed acetylene, which trimerizes above 285 K into adsorbed benzene. The benzene is stabilised on the surface by coadsorbed Cl atoms and starts to desorb from the surface above 320 K.

In this paper we report on a comprehensive study of the adsorption and reaction of *trans*-1,2-dichloroethene on CuPd(110), using molecular beam adsorption reaction spectroscopy (MBARS), temperature-programmed desorption (TPD), reflection absorption infrared spectroscopy (RAIRS), high-resolution electron energy loss spectroscopy (HREELS), and X-ray photoelectron spectroscopy (XPS).

## 2. Experimental

Three separate UHV systems were used for this study. The molecular beam and RAIRS system have been described in detail previously [14,17]. Briefly, the IR spectra were recorded at 4 $cm^{-1}$ resolution with coaddition of 256 scans using an MCT detector (spectral range 4000–650 $cm^{-1}$). The uptake is shown for the most intense cracking fragment of *trans*-1,2-dichloroethene, mass 61, whose profile is identical to that of the parent ion of mass 96 ($^{35}Cl$ isotope). A number of additional masses were also monitored for desorbing reaction products, particularly $H_2$ (mass 2), HCl (mass 36 and 38 in a 3:1 intensity ratio), $C_2H_2$ (mass 26), which are products observed from reaction of *trans*-1,2-dichloroethene on Pd(110), and benzene (mass 78) which is produced from the trimerisation reaction on Cu(110) [17]. Since mass 26 is also a cracking fragment of the parent molecule this signal contribution was subtracted to evaluate acetylene production. The only reaction products detected in the gas phase during the experiments were $H_2$, $C_2H_2$, and HCl, and therefore, only these product traces are shown.

The XPS spectra were collected on a separate system using Al-$K_\alpha$ (1486.6 eV) radiation of 140 W power (14 kV anode potential and 10 mA emission current). A multichannel HA100 VSW hemispherical analyser with an energy resolution of $\sim 2$ eV was used for analysis of the photoelectrons. Experiments were carried out following the Pd $3d_{5/2}$, Cu $2p_{3/2}$, Cl 2p, and C 1s peaks, and the elemental binding energies quoted are referenced to the Pd $3d_{5/2}$ core level at 334.9 eV from the clean CuPd(110) surface, which did not shift during the experiments. The spectra have not been deconvoluted due to the inherent complexity of the system, i.e., the two-phase binary alloy surface and the variety of dissociation products. They are simply used to support the experimental data from the other techniques to confirm the extent of dissociation.

The HREELS experiments were carried out at the CNRS in Villeurbanne, using a ELS 3000 spectrometer (LK Technologies), with additional LEED and XPS facilities. The HREELS spectrometer consists of a rotating cylindrical double-pass monochromator and a cylindrical double-pass analyser. Experiments were carried out with an incident electron beam energy of 5 eV, a resolution of $\sim 3$–4 meV, and recorded in the specular direction ($\theta_i = \theta_d = 60°$ from the surface normal). In these HREELS experiments the chromel–alumel thermocouple was attached to the sample holder, and not directly to the sample itself, as in our other experiments; this may result in a discrepancy of up to $\pm 20$ K between these experiments.

All experiments were conducted on a 50:50 CuPd(110) single crystal, an oval disk $\sim 8$ by 5 mm in size and 1.5 mm thick. Sample cleanliness was confirmed by a sharp LEED pattern prior to molecular beam and RAIRS experiments, while for XPS and HREELS experiments XPS survey scans were run to monitor carbon, nitrogen, oxygen, and sulfur impurities. The CuPd alloy can exist in two phases in the bulk, with an ordered bcc CuPd or a disordered fcc $Cu_3Pd$ structure. However, X-ray diffraction did not show the presence of the ordered bcc CuPd phase, which is expected only after very long annealing to just below 800 K [30]. It has been shown that different surface compositions of the alloy can be obtained by using different preparation procedures [31–34]. As Cu is lighter than Pd, it is preferentially sputtered from the sample in the cleaning process. However, as it is the com-

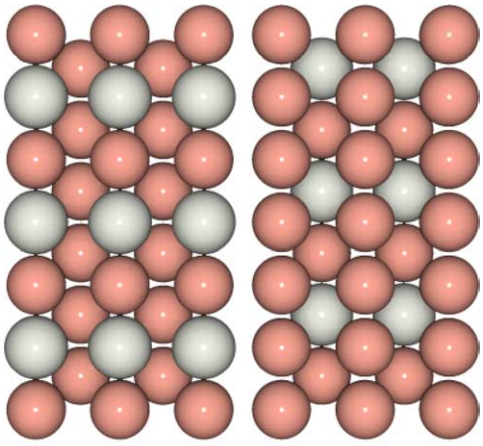


Fig. 1. The two ideal models proposed for the $Cu_3Pd(110)$ surface. In model (a) the surface terminates in a mixed Cu–Pd layer, with an all-Cu layer beneath and in model (b) the surface consists of a top layer of 100% Cu atoms, and has a mixed Cu–Pd second layer.

ponent of lower surface energy, it preferentially segregates to the surface upon annealing [35]. Enhanced segregation of Cu occurs between 700 and 825 K [31,36]; thus, it is expected that annealing the CuPd(110) sample beyond this temperature range creates a Cu-rich surface. In the experiments presented here the CuPd(110) sample was cleaned by numerous sputter cycles at 300 and 573 K (500 eV $Ar^+$, 7 μA) and then annealed to 923 K for 1 min, in order to obtain a Cu-rich surface [31–33]. Two ideal models of the $Cu_3Pd(110)$ phase have been proposed [37], in the first (Fig. 1a) the top layer consists of mixed Cu–Pd rows and the second layer contains pure Cu atoms, while the second model (Fig. 1b) consists of an all-Cu top layer with a mixed Cu–Pd layer beneath. Theoretical calculations [38] show that the surface layer containing 50% Cu and Pd atoms is a little bit more stable by 2 kJ $mol^{-1}$. A medium energy ion scattering (MEIS) study of the clean CuPd(110) surface after an identical preparation procedure [19,21] showed a Cu-rich surface, with a measured top layer composition of $Cu_{65}Pd_{35}(110)$, in good agreement with results obtained using low energy ion scattering after a similar preparation treatment [39]. Therefore, the actual PdCu(110) surface may consist of both Cu-terminated and mixed Cu–Pd-terminated terraces.

The *trans*-1,2-dichloroethene (Supelco, 99% purity) was purified using freeze-pump-thaw cycles prior to use and its purity was confirmed on admission into the chambers using mass spectrometry. For IR, HREELS, and XPS experiments it was dosed from the background through a conventional leak valve. (1 L = $10^{-6}$ Torr s.)

## 3. Results and discussion

The data from all our experiments have been summarised schematically in the reaction phase diagram in Fig. 2, showing both adsorbed and desorbing species as a function of temperature for the reaction of *trans*-1,2-dichloroethene on CuPd(110). It is clearly evident from Fig. 2 that the reactivity can be broadly categorised into two parts: Part I (85–275 K), where molecular adsorption and dissociation are observed, and where the only gas phase product is *trans*-1,2-dichloroethene. In Part II (300–925 K) gas-phase products from decomposition are observed and over this temperature range three regions of different reactivity can be identified. Therefore the data are accordingly described under these two main parts.

### 3.1. Part I: Adsorption between 85 and 275 K

#### 3.1.1. Adsorption at 85 K

Molecular beam data following the uptake of *trans*-1,2-dichloroethene on the clean CuPd(110) surface at 85 K (Fig. 3) show continuous adsorption of the molecules indicating multilayer growth. The high sticking coefficient of 0.74 remains constant throughout and is consistent with precursor-mediated adsorption, i.e., incoming molecules are trapped into a weak bound precursor state in which they diffuse over the surface until they find an adsorption site. RAIR spectra taken at 85 K (Fig. 4) confirm multilayer formation by the continual increase in intensity of the infrared bands as the surface coverage of *trans*-1,2-dichloroethene increases. There is no clear distinction between the IR bands for the monolayer and multilayer. The bands present in the multilayer (Fig. 4c) correspond closely to the most intense infrared bands observed for gas-phase *trans*-1,2-dichloroethene in the spectral range 4000–650 $cm^{-1}$ (Table 1) and show a similar intensity distribution to that obtained for *trans*-1,2-dichloroethene adsorption on Pd(110) at 85 K [14]. At this temperature the molecules are relatively weakly perturbed by the CuPd(110) substrate. The dominance of the out-of-plane $\gamma$(CH) band at 906 $cm^{-1}$ and the weakness of the in-plane $\nu$(C–Cl) and $\delta$(C–H) bands at 809 and 1197 $cm^{-1}$, respectively, suggest a general (but not strict) orientation in which the molecular planes are parallel to the metal surface, as also seen for *trans*-1,2-dichloroethene on Pd(110) [14], Cu(110) [17], Pt(110), and Pt(111) [23,25] surfaces. Upon warming, TPD data (Fig. 5) show multilayer desorption to occur at 134 K. Masses 70 ($Cl_2$), 141(PdCl), and 176($PdCl_2$) were also monitored during the TPD experiments; however, none of these species were detected, and the only other desorbing product was hydrogen (Fig. 5d).

#### 3.1.2. Molecular adsorption in the monolayer and partial dechlorination: 165 < T < 275 K

*3.1.2.1. Adsorption at low temperatures (165–175 K).* The uptake profile measured at 165 K is also shown in Fig. 3; at this temperature the surface saturates after approximately 50 s of beam exposure; for the purposes of this paper this is taken to be the saturated monolayer coverage. Although a slightly lower sticking probability is observed than at 85 K (0.70 cf. 0.74), the uptake profile is consistent with

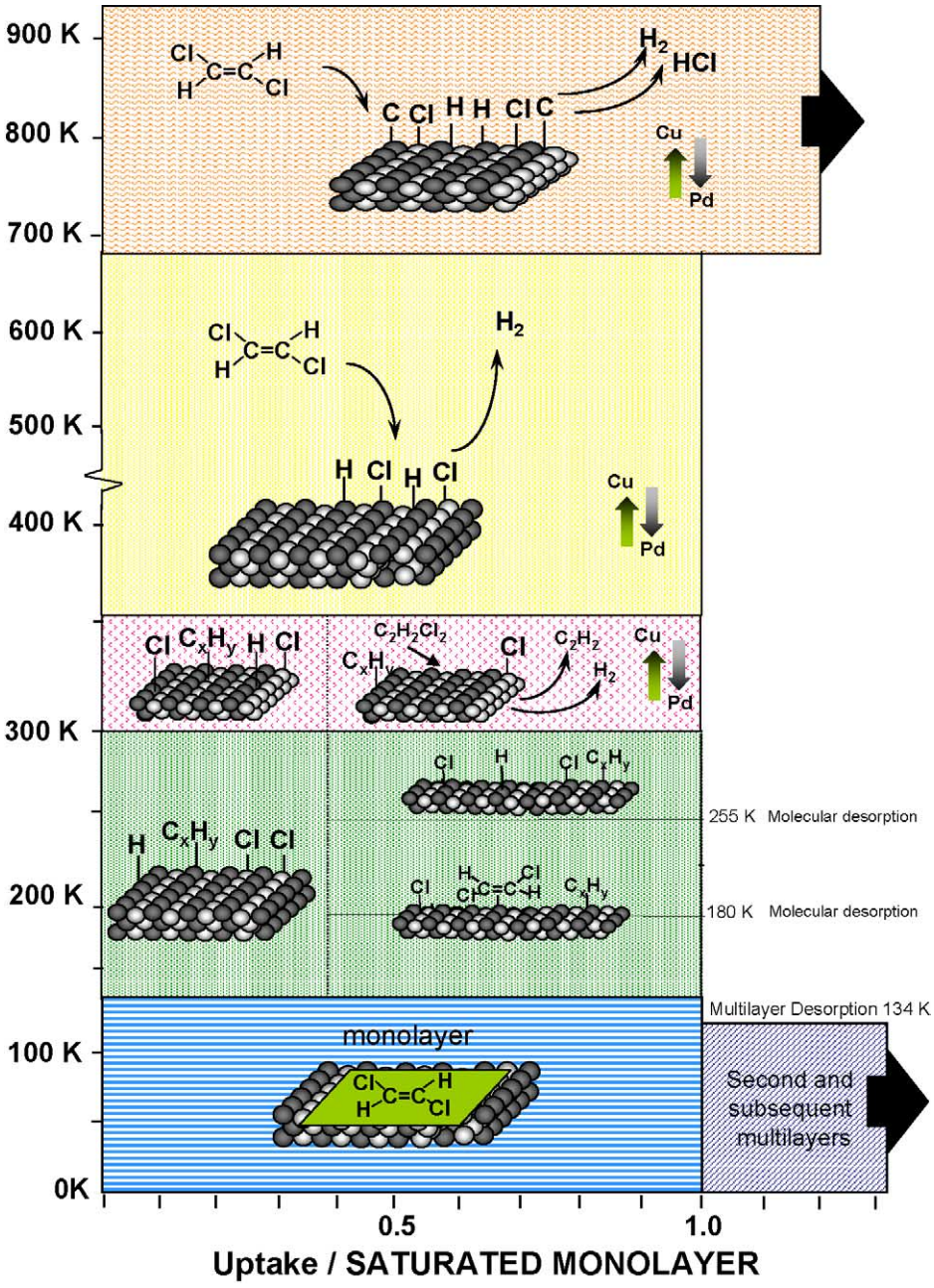


Fig. 2. Reaction phase diagram showing the reactivity of *trans*-1,2-dichloroethene on CuPd(110) as a function of temperature and reactant uptake on the surface.

precursor-mediated adsorption. No product evolution into the gas phase occurs at this temperature.

The species adsorbed on the surface have been characterised using HREELS. The spectra were recorded as a function of increasing exposure. Fig. 6 shows the EEL spectra recorded after exposures of 1 and 10 L of *trans*-1,2-dichloroethene at 180 K. The advantage of HREELS over RAIRS is the ability to measure in the low-frequency region, where metal–Cl stretches lie, which enables direct information about the onset of dechlorination processes to be obtained. The spectrum recorded after 10 L exposure (Fig. 6b) is clearly that of the molecular species, with bands between 250 and 3065 $cm^{-1}$, which are mostly associated with the fundamental molecular vibrations expected for *trans*-1,2-dichloroethene (Table 1). The bands at 1720 and 2030 $cm^{-1}$ are due to small amounts of CO produced from background adsorption. The band at 440 $cm^{-1}$ is attributed to metal–carbon stretching vibration [40] of a species produced through the initial decomposition of some of the molecules upon adsorption. The close correlation of the observed frequencies with gas-phase values demonstrates that the majority of the molecules are not strongly perturbed upon chemisorption at 180 K and retain their $\pi$-bond character. In contrast, the spectrum recorded after an exposure of 1 L *trans*-1,2-dichloroethene (Fig. 6a) shows no bands which can be correlated with molecularly adsorbed

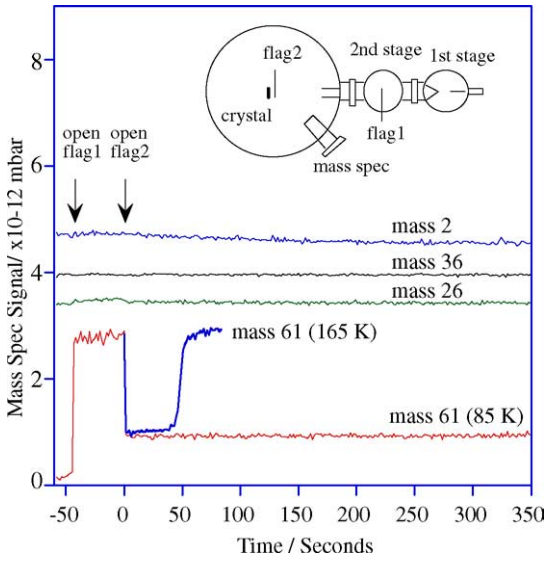


Fig. 3. Molecular beam data for the adsorption of *trans*-1,2-dichloroethene on clean CuPd(110) at 85 and 165 K. The beam of gas initially totally reflects an inert flag and strikes the crystal at time $T = 0$, as the surface saturates the signal recovers to the level off the inert flag.

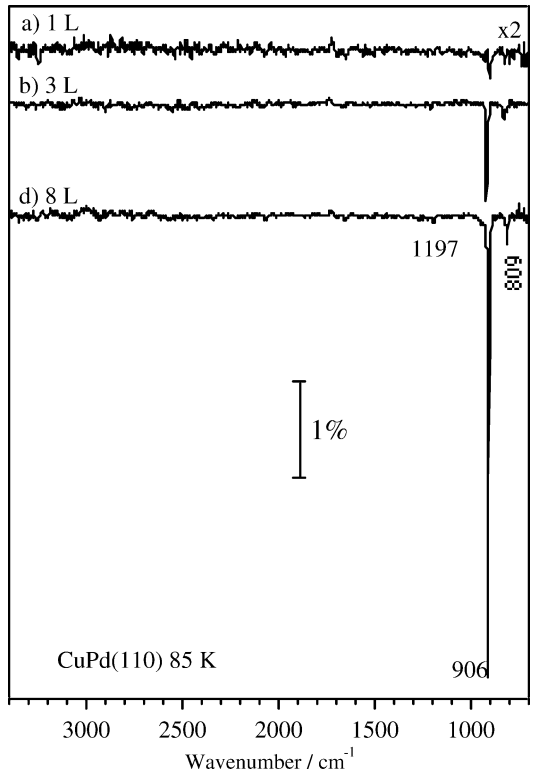


Fig. 4. RAIR spectra for adsorption of *trans*-1,2-dichloroethene adsorbed on clean CuPd(110) at 85 K as a function of increasing exposure.

*trans*-1,2-dichloroethene, indicating that initial adsorption proceeds dissociatively on the surface. Direct evidence for dechlorination of the molecules is given by the weak band at 295 $cm^{-1}$, assigned to the metal–chlorine stretching vibration [14–16,40], while the loss peak observed at 435 $cm^{-1}$ is attributed to a metal–carbon stretching vibration [40]. Further evidence in support of both dissociated and molecular species being created on the surface at low temperature is provided by XPS data, where C 1s and Cl 2p peaks show contributions from the intact molecular species and from a dechlorinated species, discussed in detail in the next section.

It is interesting to note that the vibrational spectra do not show the presence of surface acetylene which may be expected from a simple dechlorination mechanism, as observed for the interaction of *trans*-1,2-dichloroethene on Cu(110) and Pd(110) and characterised by vibrational features between 640–700, 915–940, and 1300 $cm^{-1}$ [41]. This suggests that if acetylene is produced it decomposes further or that it is not an intermediate in the decomposition process at this temperature. The small peak at 1160 $cm^{-1}$ cannot be assigned at this stage. A number of other decomposition products can be suggested; for example, Yoshinobu et al. [42] report the formation of an ethynyl (CCH) species on Pd(110) at 180 K following adsorption of low exposures of acetylene. However, none of the bands in Fig. 6a can be assigned to adsorbed ethynyl species or to other common decomposition products of acetylene such as vinyli-

Table 1
Vibrational assignments for gas- and liquid-phase *trans*-DCE [48] and frequencies observed on clean CuPd(110) at low temperatures during RAIRS and HREELS experiments, described in Part I (a) and (b)

| Assignment (gas phase) | Normal mode description | Liquid/gas-phase frequency ($cm^{-1}$) [48] | Observed frequencies ($cm^{-1}$) on CuPd(110) | |
|---|---|---|---|---|
| | | | RAIRS 85 K | HREELS 180 K |
| $\upsilon_1(A_g)$ | $\upsilon_s$(C–H) | 3073 (R) | | 3065 |
| $\upsilon_2(A_g)$ | $\upsilon$(C=C) | 1578 (R) | | 1580 |
| $\upsilon_3(A_g)$ | $\delta_s$(C–H) | 1274 (R) | | 1270 |
| $\upsilon_4(A_g)$ | $\upsilon_s$(C–Cl) | 846 (R) | | 840 |
| $\upsilon_5(A_g)$ | $\delta_s$(C–Cl) + $\delta_s$(C–H) | 350 (R) | | 350 |
| $\upsilon_6(A_u)$ | $\gamma_s$(C–H) | 895 (IR) | 906 | 905 |
| $\upsilon_7(A_u)$ | $\gamma_s$(C–Cl) − $\delta_s$(C–H) | 227 (IR) | | |
| $\upsilon_8(B_g)$ | $\tau$(HClC=CHCl) (molecular torsion) | 763 (R) | | 770 |
| $\upsilon_9(B_u)$ | $\upsilon_{as}$(C–H) | 3080 (IR) | | 3065 |
| $\upsilon_{10}(B_u)$ | $\delta_{as}$(C–H) | 1200 (IR) | 1197 | 1200 |
| $\upsilon_{11}(B_u)$ | $\upsilon_{as}$(C–Cl) | 817 (IR) | 809 | 807 |
| $\upsilon_{12}(B_u)$ | $\delta_{as}$(C–Cl) + $\delta_{as}$(C–H) | 250 (IR) | | 250 |

$\upsilon$, stretch; $\delta$, in-plane bend; $\gamma$, out-of-plane bend; $\tau$, torsion; s, symmetric; as, asymmetric; R, Raman active; IR, Infrared active.

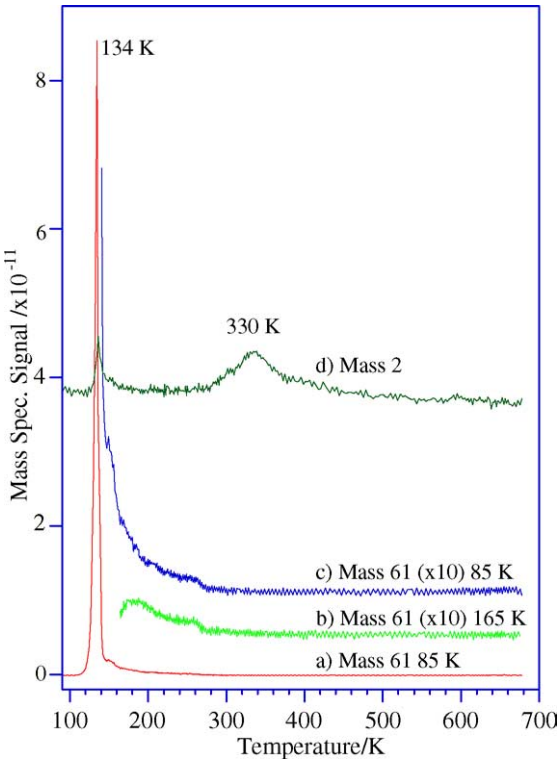


Fig. 5. TPD results taken directly after the molecular beam experiments shown in Fig. 3. (a) After exposure at 85 K, (b) exposure at 165 K, (c) expansion of 85 K data showing desorption tail of multilayer and, (d) $H_2$ evolution after both adsorption temperatures.

dene ($C{=}CH_2$) or ethylidyne ($CCH_3$) species [41–43]. We, therefore, suggest that on CuPd(110) the decomposition of the molecules upon initial adsorption has proceeded further, yielding some $C_xH_y$ fragment on the surface.

*3.1.2.2. Adsorption between 165 and 275 K.* The TPD data from a saturated overlayer formed at 165 K (Fig. 5b) show two molecular desorption states at 180 and 255 K. For additional information on the dissociation/desorption process, XPS spectra of the C 1s and Cl 2p regions were recorded after adsorption of a saturated monolayer formed at 175 K and after warming to 215, 255, 275, and 295 K (Fig. 7). At 175 K, the Cl 2p core level scan shows two distinct Cl components, a dominant peak at 201.3 eV and a smaller contribution at 198.6 eV, indicating the presence of two different states of chlorine on the surface. Each peak consists of a doublet of the Cl $2p_{1/2}$ and $2p_{3/2}$ core lines. For the higher binding energy doublet, only the $2p_{3/2}$ line at 201.3 eV is discernible, while the $2p_{1/2}$ line, expected about 1.15 eV higher in energy [25], is just visible as a broad shoulder on the high energy side of the $2p_{3/2}$ peak. The binding energy of the Cl $2p_{3/2}$ core level at 201.3 eV shows good agreement with those reported for adsorbed chlorocarbons on Pd(100) [26], Pt(111) [25,44], and Pt(110) [25] surfaces and can, therefore, be assigned to the chlorine atoms of the intact *trans*-1,2-dichloroethene. An indication of some initial dechlorination is revealed by the presence of the peak

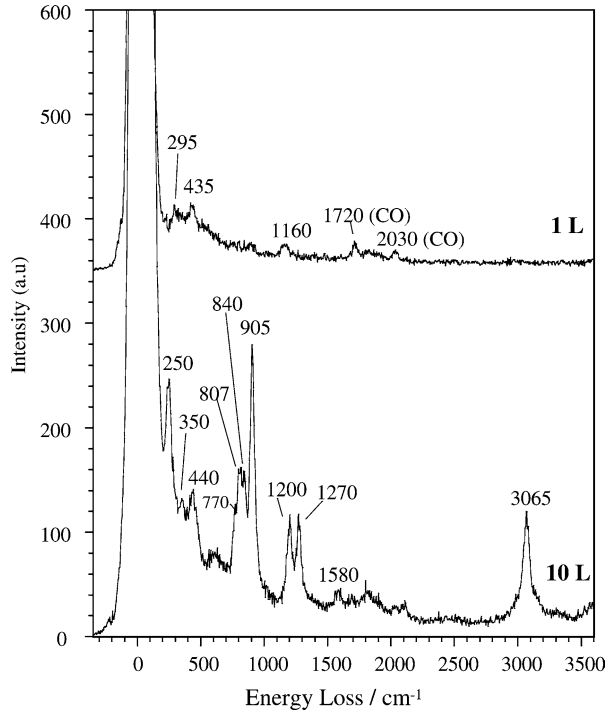


Fig. 6. HREEL spectra obtained following adsorption of (a) 1 L and (b) 10 L *trans*-1,2-dichloroethene onto CuPd(110) at 180 K. Bands between 1720 and 2100 $cm^{-1}$ are due to adsorbed CO impurity.

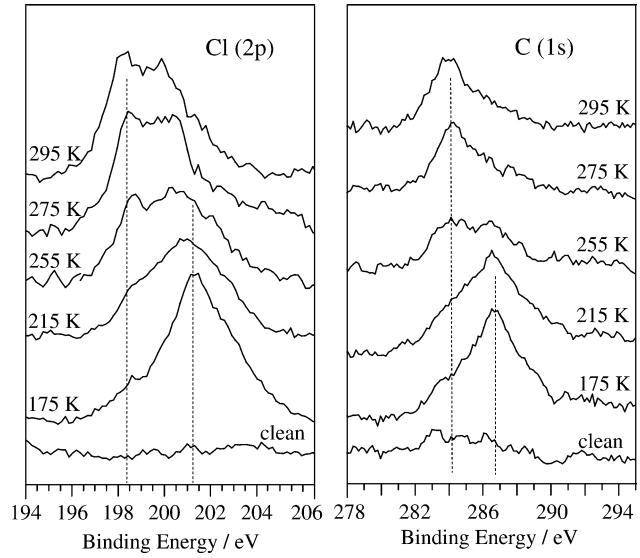


Fig. 7. X-ray Photoelectron (XP) spectra obtained following (a) the Cl 2p and (b) C 1s peaks, after exposure of 40 L *trans*-1,2-dichloroethene onto clean CuPd(110) at 175 K and subsequent warming.

located at 198.6 eV, which, through comparison with binding energies reported for the adsorption of chlorine gas on the Pt(111) surface [44], can be attributed to the Cl $2p_{3/2}$ line of adsorbed Cl atoms on the CuPd(110) surface. The $2p_{1/2}$ line of this Cl 2p doublet is not resolvable in the spectrum as it is hidden by the intense Cl $2p_{3/2}$ peak of the chlorine on the intact molecules. The C 1s core level scan obtained at this temperature (Fig. 7b) can also be resolved into two peaks:

a dominant peak at 286.6 eV and a smaller peak at 284 eV. Since Cl substituents in adsorbed hydrocarbons are known to shift the binding energy of the C 1s core level to higher values, these two peaks can be assigned, respectively, to carbon in molecular *trans*-1,2-dichloroethene and carbon from an adsorbed hydrocarbon species, produced through decomposition [25,26,44,45]. The combination of HREELS and XPS data indicates that the saturated monolayer formed at 175 K mainly consists of intact molecules, and that only a fraction of the molecules undergo C–Cl bond cleavage to give adsorbed chlorine and an intermediate hydrocarbon species.

As the sample is warmed to 215 and 255 K the Cl $2p_{3/2}$ peak at 198.6 eV (Fig. 7a) grows in intensity, while the higher binding energy $2p_{3/2}$ line due to intact molecules decreases. This indicates dissociation of C–Cl bonds and is further confirmed by the growth of the 284 eV feature in the C 1s spectrum (Fig. 7b). Finally, further heating to 275 K results in the almost complete attenuation of the C 1s peak at 286.6 eV and Cl $2p_{3/2}$ component at 201.3 eV, associated with the intact *trans*-1,2-dichloroethene molecules, suggesting that desorption/dechlorination of the majority of molecules has occurred by this temperature.

These XPS data suggest that the molecular desorption profile observed in Fig. 5b is due to competitive desorption/dechlorination processes which occur with increasing temperature. Thus some molecular desorption is first seen to occur at 180 K in the TPD, while XPS data obtained at 175 and 215 K reveal that this desorption process is accompanied by dechlorination of some of the remaining adsorbed molecules, presumably at the vacant sites produced by the desorbing molecules. XPS data also reveal that a substantial molecularly adsorbed phase remains and we suggest that Cl atoms created in the dechlorination process serve to stabilise remaining molecules of intact *trans*-1,2-dichloroethene, preventing their further desorption/decomposition. As a result, the rate of desorption and, hence, dechlorination decreases until higher temperatures, resulting in a second molecular desorption state at 255 K. At this temperature XPS data record an increase in dechlorination of the remaining molecules, leaving adsorbed Cl and other hydrocarbon fragments on the surface. We note that similar self-poisoning desorption/dissociation behaviour has been previously reported on the Cu(110) surface following reaction with a variety of chloroethenes [17]. Unfortunately on the CuPd(110) surface no conclusive spectroscopic evidence is available to identify the hydrocarbon decomposition products. No chlorine-containing desorption products desorb from the surface, and the adsorbed Cl remains bound to the CuPd(110) surface up to 600 K.

To summarise the adsorption between 165 and 275 K, we conclude that in the early stages of adsorption, the molecules of *trans*-1,2-dichloroethene decompose at the surface to produce C, Cl, and $C_xH_y$ species. However, as adsorption proceeds, the surface activity is suppressed by C, Cl, and $C_xH_y$ accumulation, inhibiting dissociation and leading to intact molecular adsorption. The initial high activity of the CuPd(110) surface is similar to that observed on Pd(110) [14]; however, differences are noted in the behaviour at high uptakes. On Pd(110) deposition of adsorbed $C_x$ and Cl species leads to inhibition of C–H and C–C bond cleavage, but dissociation of the C–Cl bonds remains unaffected and adsorbed acetylene is produced, which dissociates/desorbs above 250 K. On Cu(110) the decomposition exclusively produces an adsorbed di-$\sigma$/di-$\pi$-bonded acetylene species between 220 and 266 K, above which it begins to trimerise into benzene. Therefore, over this temperature range the chemistry of the alloy differs from that of the individual metals in that if the acetylene intermediate is formed it is not stabilised to the same extent.

### *3.2. Part II: Adsorption and reaction between 300 and 925 K*

The extent of dissociation above 300 K has been followed using a combination of HREELS and XPS, both of which show that the reaction of *trans*-1,2-dichloroethene with the alloy surface above 300 K leads to the complete dissociation of the molecules. After a saturation exposure at 300 K, the XP spectra of the Cl 2p region show a main peak at 198.4 eV with a shoulder at 199.9 eV (Fig. 8a) consistent with the presence of only atomic Cl [44]. Similarly in the C 1s region (Fig. 8b) a peak at 283.8 eV demonstrates that no chlorocarbon is present on the surface. The HREEL spectrum after a saturation exposure at 300 K (Fig. 9) shows a dominant loss peak at 320 $cm^{-1}$. This is assigned to $\nu$(M–Cl) of atomic Cl on the alloy surface. The frequency of this band can be used to determine to which of the two metals on the alloy surface the Cl is bonded [28]. The $\nu$(M–Cl)

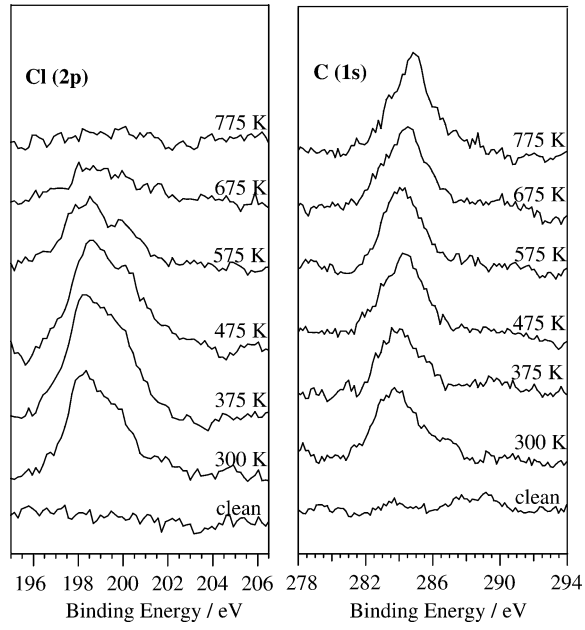


Fig. 8. XPS data obtained following adsorption of 40 L *trans*-1,2-dichloroethene on CuPd(110) surface at 300 K and subsequent thermal treatment, following (a) the Cl 2p and (b) C 1s peaks.

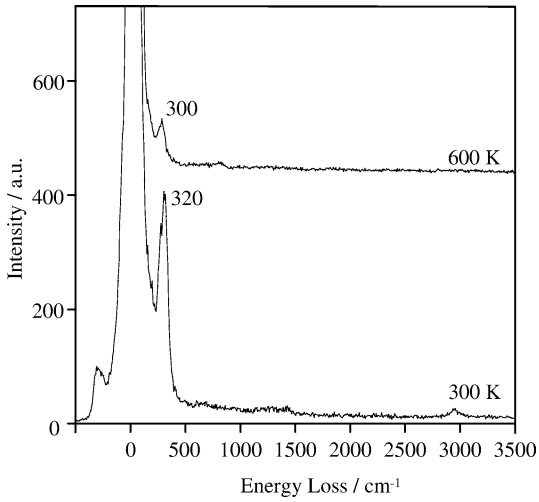


Fig. 9. HREEL spectra obtained following adsorption of 10 L *trans*-1,2-dichloroethene onto clean CuPd(110) at 300 K and after warming to 600 K.

frequency has been measured to be 270 and 315 $cm^{-1}$ for atomic Cl produced from the decomposition of *trans*-1,2-dichloroethene on Pd(110) and Cu(110), respectively. Therefore, it would appear that the Cl atoms created in the dechlorination process preferentially bind to the Cu atoms on the alloy surface. This supports previous MEIS results for this system, which showed an enrichment of Cu atoms in the topmost layer, and a concomitant decrease of Cu in the second layer. This dynamic interchange in the Cu content between the top two layers suggests that to some degree the alloy composition is maintained as Cu–Cl islands grow. From a simple thermodynamic point of view this process is driven by the higher enthalpy of Cu–Cl bond formation compared to Pd–Cl bond formation ($\Delta H_f$ (Cu–Cl) $= -328$ kJ $mol^{-1}$ and $\Delta H_f$ (Pd–Cl) $= -271.7$ kJ $mol^{-1}$ [46]). Detailed theoretical DFT calculations show that the mechanism for this derives from the adsorption geometry in the transition state prior to decomposition, where strong Pd–C and Cu–Cl bonds are formed [27–29]. Importantly the preferential formation of Cu–Cl islands indicates that the Pd sites in the alloy are kept free of Cl and, therefore, should show different reactivity to that observed on Pd{110} at high uptake values when coadsorbed Cl significantly affects the surface chemistry. We have investigated if the reactivity of the CuPd alloy is changed in this manner by following the desorption products in temperature-dependent molecular beam experiments on the alloy surface and comparing these to those previously measured on Cu{110} and Pd{110} surfaces.

The molecular beam data measured between 300 and 925 K (Fig. 10) show that the uptake and product evolution into the gas phase is strongly temperature dependent. Over this temperature range the initial sticking coefficient changes slightly from 0.64 to 0.55 and the uptake, which at 300 K is 60% of that measured at 165 K, now increases above 475 K. The reactivity can be broadly categorised into three temperature regimes. The first, between 310 and 355 K, shows the simultaneous evolution of $H_2$ and $C_2H_2$. In the

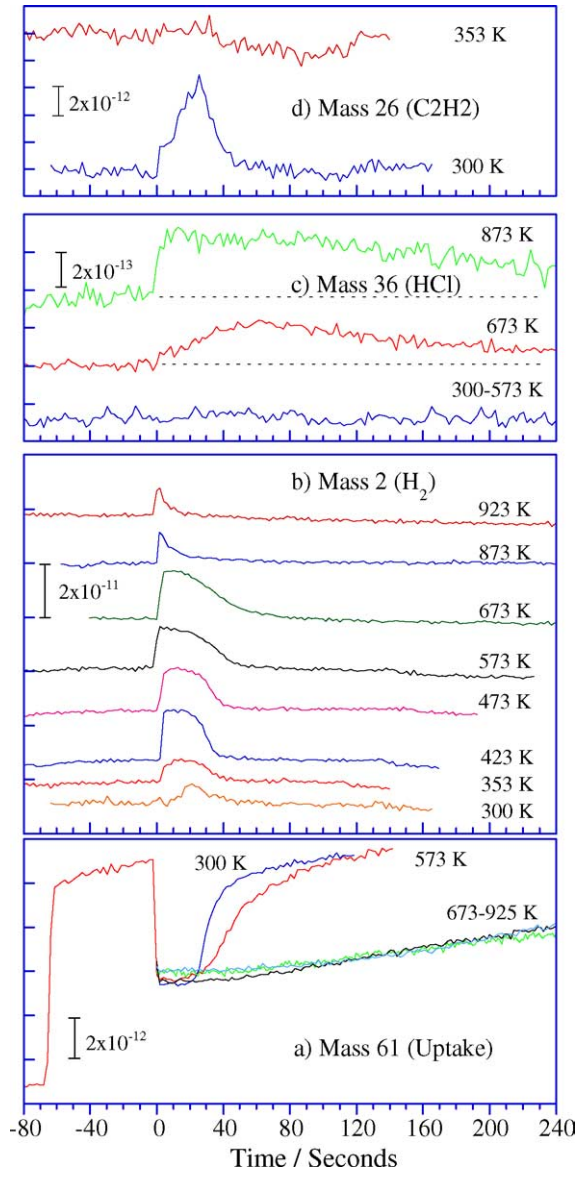


Fig. 10. Molecular beam data of *trans*-1,2-dichloroethene on CuPd(110) measured between 300 and 925 K. The progress of the reaction is followed using the uptake profile of the molecular ion (mass 61). The evolution of the main products: $H_2$ (mass 2), HCl (mass 36), and $C_2H_2$ (mass 26) are only shown at temperatures where changes are observed.

second, above 355 K, only desorbing $H_2$ is observed, and finally above 670 K a pseudo-steady-state reaction producing HCl begins. We note that in these experiments no benzene was observed, which is produced with high selectivity from the trimerisation of the acetylene intermediate from the reaction of *trans*-1,2-dichloroethene on Cu(110), thus excluding chemistry from Cu-rich terraces. To understand the influence of Cu and Pd in the alloy surface on the mechanisms responsible for the evolution of these products we proceed by comparing the results from the alloy with those observed on Cu(110) and Pd(110). Fig. 11 shows a schematic summary of all the species observed from the reaction of *trans*-1,2-dichloroethene on Cu(110), Pd(110) and CuPd(110) surfaces

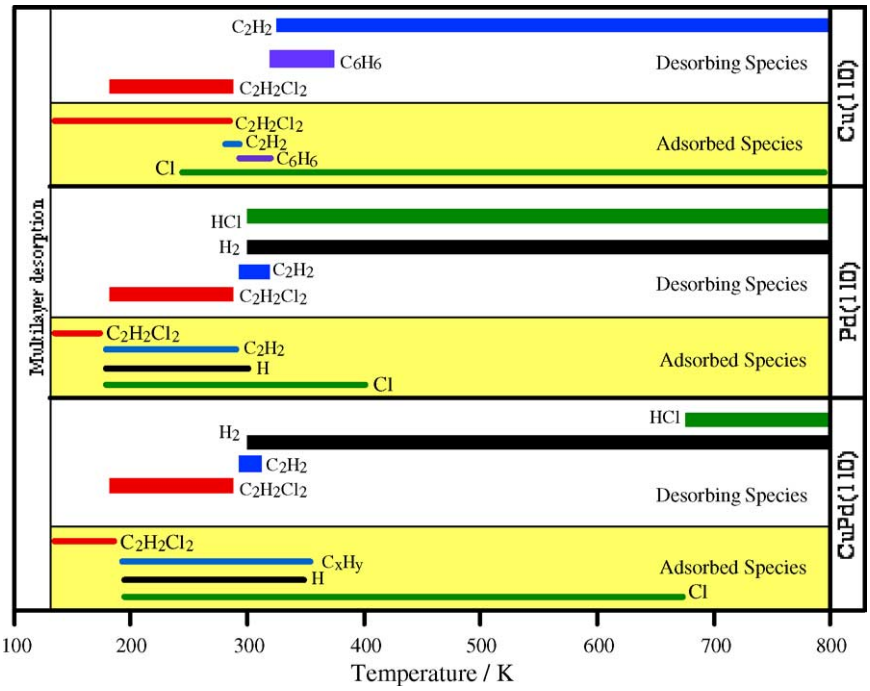


Fig. 11. Schematic summary of adsorbed and desorbing species from the reaction of *trans*-1,2-dichloroethene on CuPd(110), Pd(110), and Cu(110) surfaces.

between 100 and 800 K, and includes both adsorbed and desorbing species

### 3.2.1. 300–355 K: Reaction with $H_2$ and $C_2H_2$ evolution

The data over the small temperature range of 300–350 K show a set of differences for the CuPd surface with respect to the pure metals and provide some insight into how these metals direct the surface chemistry on the alloy surface. Fig. 12 shows in detail the molecular beam data measured at 300 K, together with our previous results from Pd(110). The reaction on the Cu(110) surface showed no desorbing products at 300 K (and therefore the data are not shown), although adsorbed benzene produced by the trimerisation of acetylene was observed with RAIRS. The data from the Pd(110) surface were interpreted as follows. Initial total decomposition at 300 K leads to recombinative $H_2$ desorption. After a critical uptake, adsorbed $C_xH_y$ and Cl species poison the surface toward further C–H bond cleavage. This results in a change of decomposition mechanism leading to the production of gaseous $C_2H_2$ and HCl, the latter formed by the reaction of surface H with Cl (either from the surface or from some reactive intermediate). In contrast, the CuPd surface shows the simultaneous production of $H_2$ and $C_2H_2$, but no HCl. The evolution of $H_2$ is only observed from the reaction of *trans*-1,2-dichloroethene with Pd(110), and is never observed with Cu(110). This implies that over the temperature and coverage range where $H_2$ is observed as a reaction product from the alloy surface, Pd atoms must be present in the topmost layer and that their activity toward breaking the C–H bonds is relatively unchanged by alloying with Cu, in agreement with recent DFT calculations [27–29]. Therefore, using the results from XPS and HREELS the molecular

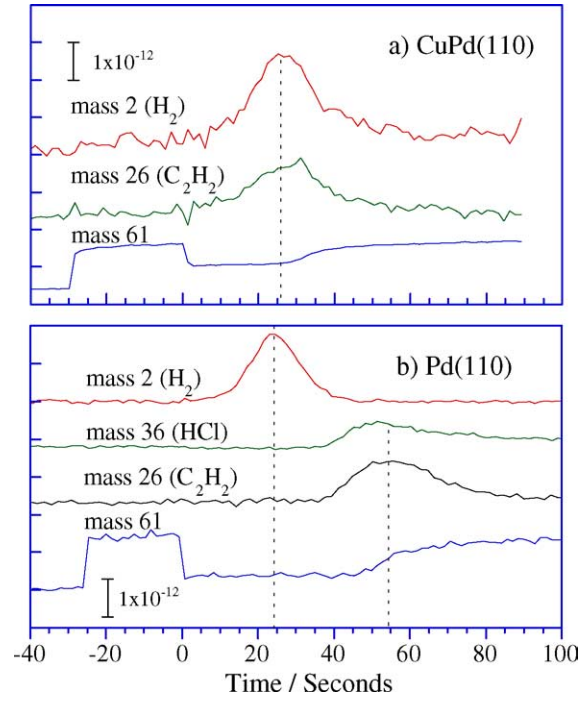


Fig. 12. Comparison of molecular beam data for adsorption of *trans*-1,2-dichloroethene on (a) CuPd(110) and (b) Pd(110) at 300 K.

beam data measured at 300 K can be interpreted as follows. Initial interaction leads to total decomposition into atomic H, Cl, and C, the Cl preferentially reacting with Cu to form Cu–Cl islands. After a critical coverage of these species the atomic H is destabilised and desorbs, and there is a change in the reaction mechanism where only dechlorination occurs, producing acetylene which immediately desorbs. Eventu-

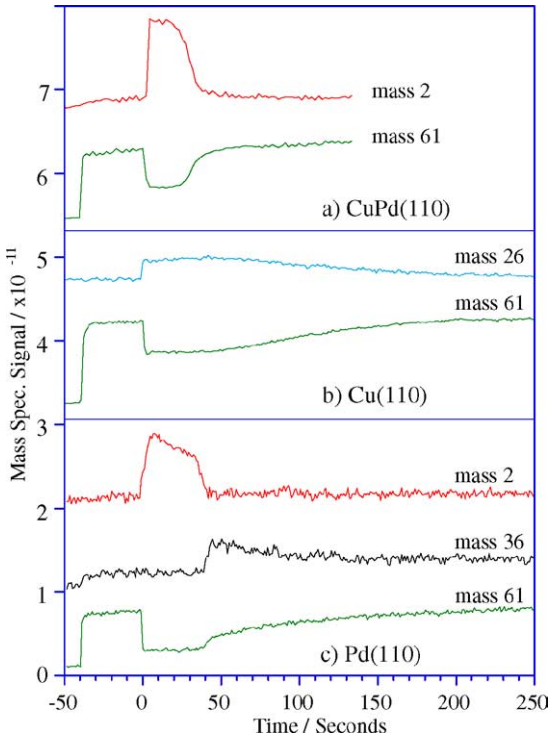


Fig. 13. Comparison of molecular beam data for adsorption of *trans*-1,2-dichloroethene on (a) CuPd(110), (b) Cu(110), and (c) Pd(110) at 425 K.

ally, the reaction is terminated as the surface is poisoned with contaminants left behind from the decomposition process.

The above results appear to indicate that the decomposition of the hydrocarbon skeleton is mainly at Pd sites and the activity of the Cu is suppressed by its reaction with Cl to form Cu–Cl. Additional support for this comes from comparison of higher temperature data from Cu, Pd, and CuPd (110) surfaces, e.g., at 425 K (Fig. 13). At this temperature if Cu chemistry were sustained then some acetylene would be observed. Instead only $H_2$ is observed throughout the uptake (Fig. 13a), which is very similar to the result from Pd(110) (Fig. 13c), albeit with the absence of HCl. Between 355 and 673 K, the desorbing $H_2$ appears from the onset of adsorption and continues throughout the uptake, as in this temperature range atomic H is not stable on the surface and desorbs as $H_2$ immediately on formation.

### 3.2.2. $355 < T < 670$ K: Reaction with $H_2$ evolution

Between 355 and 670 K only hydrogen is evolved from the surface, which is unusual with respect to the reactivity of Cu(110) and Pd(110) surfaces, as shown in Fig. 13 for adsorption at around 425 K. On the Pd(110) surface after the initial $H_2$ evolution of HCl is observed, while on Cu(110) only acetylene is observed over the entire uptake. The production of HCl on Pd(110) only starts after significant accumulation of C and Cl contaminants, which act to lower the activation energy barrier for HCl formation and desorption [14]. Importantly, experiments with preadsorbed C and Cl on Pd(110) showed that whereas C inhibited HCl production, preadsorbed Cl promoted its production [14]. The reaction kinetics on CuPd(110) are entirely different due to the preferential reaction of Cl with Cu, and it is the stability of the Cu–Cl surface layer that determines the uptake and reaction products. It should be noted that in the case of the Cu(110) the sticking probability, and hence acetylene production, rapidly diminishes above 500 K, whereas it is unchanged for Pd(110). The uptake increases significantly above 400 and 573 K for Pd(110) and CuPd(110), respectively. As $H_2$ is the only desorption product above 355 K the increase in uptake above 573 K on the alloy suggests a change in the surface composition of the C and Cl contaminants. The XPS data of the Cl 2p region after saturation of the surface at 300 K and annealing to higher temperature (Fig. 8a) show that as the temperature is raised above 575 K the intensity of the Cl 2p lines due to adsorbed chlorine at 198.4 and 199.9 eV decreases in intensity, indicating a reduction in surface chlorine. The HREEL spectra also show a reduction of the $\nu$(C–Cl) peak at 310 $cm^{-1}$ peak (Fig. 9). The mechanism for this is not clear as we are unable to detect any Cl-containing desorption products; one possible explanation is diffusion of Cl into the bulk. In contrast, the C 1s spectrum (Fig. 8b) shows no change over this temperature range, which indicates that the carbon overlayer formed at 300 K is relatively more stable.

### 3.2.3. $T > 670$ K: Reaction with HCl evolution

Above 670 K, HCl evolution is observed. At 673 K, the initial $H_2$ production gradually gives way to HCl production, similar to that observed on Pd(110) at 300 K. At 825 K a pseudo-steady-state reaction occurs on the CuPd(110) surface in which incoming molecules are continually converted to HCl, with a considerable increase in uptake of the reactants on the surface. We note on Pd(110) that this process is observed to start much earlier at 410 K. The absence of carbon-containing desorption products suggests that the excess carbon produced from the decomposition over this temperature range must be absorbed into the bulk. The difference between the pure Pd and the alloy surface is the stability of the Cl: on Pd it readily reacts with H to form HCl, whereas on the alloy the Cl preferentially binds to the Cu, and thus the stability of the Cu–Cl determines the likelihood of any further reaction. For example, on Cu(110), the reaction mechanism with 1,1-dichloroethene is significantly different than with 1,2-dichloroethene in that it totally decomposes, and the atomic H and Cl react to produce HCl above 650 K [47]. Therefore, under these conditions Cu–Cl can be reduced by the presence of atomic H, which is clearly produced as a decomposition product on the alloy surface. It has previously been reported that above 700 K enhanced Cu segregation occurs [31,36], leading to nearly all the atoms in the top rows of the (110) surface to be Cu, while the atoms in the troughs are Pd. Therefore, for the dissociative reaction that we observe here, there is either a significant number of Pd atoms remaining in the topmost layer or the Pd atoms in the troughs are readily accessible for reaction with the incident molecules. Although, we do note that unlike the re-

action on Pd(110) true steady state is not achieved as the uptake gradually decreases, presumably due to a lack of Pd sites due to changes in surface composition caused by extensive Cu segregation.

## 4. Overall conclusion

In summary, the adsorption and reaction of *trans*-1,2-dichloroethene on CuPd(110) between 85 and 923 K has been shown to be strongly temperature dependent. Decomposition begins in the early stages of adsorption at 180 K, and is found to be temperature and coverage dependent due to the availability of surface sites and stabilisation by coadsorbed Cl produced from initial decomposition. Above 300 K the main desorbing reaction products are $H_2$, $C_2H_2$, and HCl, the ratio of these again being dependent on surface coverage and temperature. Between 300 and 355 K initial adsorption onto the alloy surface leads to total decomposition to yield H, Cl, and $C_x$ species. With increasing uptake the H atoms combine and desorb as $H_2$, and the decomposition mechanism changes to produce acetylene through selective dechlorination, which desorbs on formation. Between 355 and 675 K total decomposition is observed leading to the exclusive evolution of $H_2$; the reaction of H and Cl to produce HCl only begins at above 670 K. The Cl preferentially binds to the Cu atoms, which leads to dynamic changes in the composition of the alloy surface with segregation of Cu from underlying layers to the surface. This results in significantly different reaction chemistry than that observed with the pure metals. These results are entirely consistent with recent DFT calculations [27–29], which show that the decomposition of chloroethenes is at Pd sites on the alloy surface, the reactivity of which is similar to that of the Pd(110) surface. However, unlike the reaction on the Pd(110) surface HCl production is only observed above 670 K; this is attributed to the stability of Cu–Cl below this temperature.

## Acknowledgments

This work was done within the European Associated Laboratory context supported by EPSRC and CNRS. We are grateful for their financial contribution for equipment grants and a postdoctoral fellowship to S.H., and to ICI Chlor-Chemicals and ICI Klea for a CASE award for L.B. We thank Drs. C. Mitchell and N. Winterton for useful discussions, and Dr. P. Sautet for forwarding his research results prior to publication.

## References

[1] S.C. Fung, J.H. Sinfelt, J. Catal. 103 (1987) 220.
[2] S.C. Chuang, J.W. Bozzelli, Environ. Sci. Technol. 20 (1986) 568.
[3] L.S. Vadlamannati, V.I. Kovalchuk, J.L. d'Itri, Catal. Lett. 58 (1999) 173.
[4] L.J. Matheson, P.G. Tratneyk, Environ. Sci. Technol. 28 (1994) 2045.
[5] C.W. Chen, A.J. Gellman, Catal. Lett. 53 (1998) 139.
[6] G. Rupprechter, G.A. Somorjai, Catal. Lett. 48 (1997) 17.
[7] E.R. Ritter, J.W. Bozzelli, A.M. Dean, J. Phys. Chem. 94 (1990) 2493.
[8] A.H. Weiss, S. Valinski, J. Catal. 74 (1982) 136.
[9] V.N. Romannikov, K.G. Ione, Kinet. Catal. 25 (1984) 75.
[10] C.F. Ng, C.K. Chan, J. Catal. 89 (1984) 553.
[11] C.F. Ng, K.S. Leung, C.K. Chan, J. Catal. 78 (1982) 51.
[12] A.H. Weiss, K.A. Krieger, J. Catal. 6 (1966) 167.
[13] R. Ohnishi, W.L. Wang, M. Ichikawa, Appl. Catal. A 113 (1994) 29.
[14] L.H. Bloxham, S. Haq, C. Mitchell, R. Raval, Surf. Sci. 489 (2001) 1.
[15] Y. Jugnet, N.S. Prakash, J.-C. Bertolini, S.C. Laroze, R. Raval, Catal. Lett. 56 (1998) 17.
[16] S.C. Laroze, S. Haq, R. Raval, Y. Jugnet, J.-C. Bertolini, Surf. Sci. 433–435 (1999) 293.
[17] S. Haq, S.C. Laroze, C. Mitchell, N. Winterton, R. Raval, Surf. Sci. 531 (2003) 145.
[18] S. Haq, S.C. Laroze, C. Mitchell, N. Winterton, R. Raval, in: S.D. Jackson, D. Lennon, J.S.J. Hargreaves (Eds.), Catalysis in Application, Royal Society of Chemistry, 2003, p. 121.
[19] C.J. Baddeley, L.H. Bloxham, S.C. Laroze, R. Raval, T.C.Q. Noakes, P. Bailey, Surf. Sci. 433–435 (1999) 827.
[20] T.C.Q. Noakes, P. Bailey, S.C. Laroze, L.H. Bloxham, R. Raval, C.J. Baddeley, Surf. Interface Anal. 30 (2000) 81.
[21] C.J. Baddeley, L.H. Bloxham, S.C. Laroze, R. Raval, T.C.Q. Noakes, P. Bailey, J. Phys. Chem. B 105 (2001) 2766.
[22] M.X. Yang, P.W. Kash, D.-H. Sun, G.W. Flynn, B.E. Bent, M.T. Holbrook, S.R. Bare, D.A. Fischer, J.L. Gland, Surf. Sci. 380 (1997) 151.
[23] V.H. Grassian, G.C. Pimentel, J. Chem. Phys. 88 (1997) 4478.
[24] V.H. Grassian, G.C. Pimentel, J. Chem. Phys. 88 (1997) 4484.
[25] A. Cassuto, M.B. Hugenschmidt, Ph. Parent, C. Laffon, H.G. Tourillon, Surf. Sci. 310 (1994) 390.
[26] K.T. Park, K. Klier, C.B. Wang, W.X. Zhang, J. Phys. Chem. B 101 (1997) 5420.
[27] L.A.M.M. Barbosa, D. Loffreda, P. Sautet, Langmuir 18 (2002) 2625.
[28] Y. Jugnet, J.C. Bertolini, L.A.M.M. Barbosa, P. Sautet, Surf. Sci. 505 (2002) 153.
[29] L.A.M.M. Barbosa, P. Sautet, J. Catal. 207 (2002) 127.
[30] R. Hultgren, et al., Selected Values of the Thermodynamic Properties of Binary Alloys, American Society for Metals, Metals Park, OH, 1973.
[31] J. Loboda-Cackovic, M.S. Mousa, J.H. Block, Vacuum 46 (1995) 89.
[32] J. Loboda-Cackovic, Vacuum 47 (1996) 1405.
[33] J. Loboda-Cackovic, Vacuum 48 (1997) 571.
[34] A. Rochefort, M. Abon, P. Delichere, J.-C. Bertolini, Surf. Sci. 294 (1993) 43.
[35] M.A. Newton, S.M. Francis, M. Bowker, Surf. Sci. 259 (1991) 56.
[36] J. Loboda Cackovic, M.S. Mousa, J.H. Block, Vacuum 46 (1995) 117.
[37] L. Lianos, Y. Debauge, J. Massardier, Y. Jugnet, J.-C. Bertolini, Catal. Lett. 44 (1997) 211.
[38] V. Ledentu, P. Sautet, private communication.
[39] Y. Debauge, M. Abon, J.-C. Bertolini, J. Massardier, A. Rochefort, App. Surf. Sci. 90 (1995) 15.
[40] See, for example, H. Ibach, D.L. Mills, Electron Energy Loss Spectroscopy and Surface Vibrations, Academic Press, San Diego, 1982.
[41] N. Sheppard, Annu. Rev. Phys. Chem. 39 (1988) 589.
[42] J. Yoshinobu, T. Sekitani, M. Onchi, N. Nishijima, J. Electr. Spectrosc. Rel. Phenom. 54/55 (1990) 697.
[43] J.A. Gates, L.L. Kesmodel, Surf. Sci. 124 (1983) 68.
[44] F. Steinbach, J. Kiss, R. Krall, Surf. Sci. 157 (1985) 401.
[45] N. Freyer, G. Pirug, H.P. Bonzel, Surf. Sci. 126 (1983) 487.
[46] D.R. Lide (Ed.), Handbook of Chemistry, Physics, seventy seventh ed., CRC Press, Boca Raton, FL, 1997.
[47] S. Haq, S.C. Laroze, C. Mitchell, N. Winterton, R. Raval, in preparation.
[48] K.S. Pitzer, J.L. Hollenberg, J. Am. Chem. Soc. 76 (1954) 1493.